



A STUDY OF THE EFFECT OF THE PULSATILE VENTRICULAR PRESSURE IN THE DEVELOPMENT OF HYDROCEPHALUS

Jason Fritz¹, Corina Drapaca¹

¹ The Pennsylvania State University, University Park, USA, jsf186@psu.edu, csd12@psu.edu

Abstract: Hydrocephalus is a condition which occurs when an excessive accumulation of cerebrospinal fluid in the brain causes enlargement of the ventricular cavities. Although known instances of hydrocephalus date back to the time of Hippocrates, the process by which hydrocephalus develops is still not well understood. Recently, the pulsations of the cerebrospinal fluid due to the heartbeats have been suggested as a possible mechanism causing ventricular expansion. The aim of the present paper is to study the changes in the brain geometry due to the ventricular deformations caused by the pulsatile ventricular pressure. In our model, we used the real geometry of the brain taken from MR images and we assumed that the brain parenchyma behaves as a non-linear hyper-elastic solid. Our results show that our model is able to correctly predict the large displacements seen in hydrocephalic brains. To the best of our knowledge, this is the first time such a model has been used for modeling, simulating, and studying hydrocephalus.

Keywords: Hydrocephalus, Brain Biomechanics, Hyperelastic Solid, Abaqus

1. INTRODUCTION

Hydrocephalus is a clinical condition characterized by abnormalities in the cerebrospinal fluid (CSF) circulation, resulting in ventricular dilation (Figure 1). Normally, there is a delicate balance between the rate of formation and of absorption of CSF, the entire volume being absorbed and replaced once every twelve to twenty-four hours [23]. The CSF forms within the lateral ventricles of the brain, circulates through the ventricles and within the subarachnoid space surrounding the brain, and drains into the venous blood by passing through the arachnoid villi located in the dura matter above the brain [18]. The driving forces to convey the CSF out of the ventricular system are: the pressure gradients between the different parts of the ventricular system, the subarachnoid space, and the venous sinuses [8]. These pressure gradients are created by the continuous CSF secretion and are enhanced by the arterial pulsations of the brain with each heartbeat.

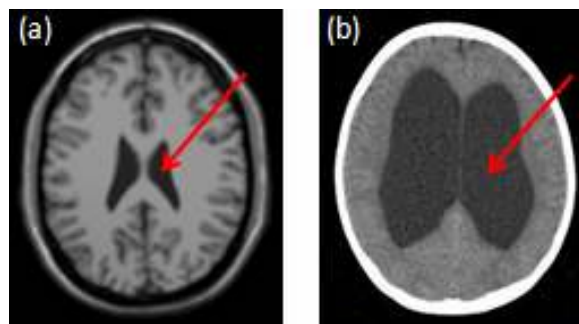


Figure 1: (a) MRI image of a normal brain [10]. (b) CT image of a hydrocephalic brain [12]. Ventricles are indicated by red arrow.

Although hydrocephalus cases were regularly described by Hippocrates (466-377 B.C.) and Galen (130-200 A.D.), the first detailed description of a treatment was given in the tenth century by Abulkassim Al Zahrami [2]. Still another six centuries had to pass for the first clear description of hydrocephalus to be given by Vesalius (1514-1564), and only recently has its treatment started to be more successful [6]. Currently, it is believed that hydrocephalus may be caused by increased CSF production, by obstruction of CSF circulation or of the venous outflow system [8], or due to genetic factors [33].

One possible, age-related, classification of hydrocephalus is into infantile and normal pressure (NPH) hydrocephalus. In the infantile hydrocephalus, the intracranial pressure is raised, and, as the CSF accumulates in the ventricles, the brain tissue compresses, and both the ventricles and the skull, enlarge. On the other hand, NPH is predominantly found in adults over 60 years of age, and it is characterized by a normal intraventricular pressure. Unlike the infantile type, NPH is hard to diagnose since many conditions affecting older individuals can mimic the symptom profile of NPH, including Parkinson's disease, Alzheimer's disease, metabolic and psychiatric disorders, endocrine dysfunction, infections, trauma, vascular and neurodegenerative disorders, and incontinence from urinary tract disorders [25]. The efforts in treatment have been principally through CSF flow diversion. Within limits, the dilation of the ventricles can be reversed by either implanting a CSF shunt or by performing an endoscopic third ventriculostomy surgery, resulting in a relief from the symptoms of hydrocephalus. However, despite the efforts of neurosurgeons and great advances in technology, the two treatment options display no statistically significant difference in the efficacy for treating hydrocephalus because the process by which hydrocephalus develops is still poorly understood.

In order to better understand the pathophysiology of hydrocephalus, appropriate mathematical and computational models are required. So far, there have been two approaches to modeling the biomechanics of the hydrocephalic brain parenchyma. In the first approach the brain is modeled as a linear elastic or viscoelastic material [9,17,19,20,30,31]. In the second approach, the brain parenchyma is assumed to be made of a porous, linearly elastic solid with Newtonian fluid filled pores [15,22,24,26,27,28]. Both linear viscoelastic and poroelastic models are based on the assumption of small strain theory which means that they are capable to predict only small deformations. To correctly model the large deformations seen in hydrocephalus, a nonlinear material law is required. The first quasi-linear viscoelastic model of the brain parenchyma was proposed in [7]. However, all the above mentioned mechanical models suffer from the assumption that the brain's geometry is either a cylinder or a sphere. In addition, with the exception of the models presented in [28] and [31], none of the other models takes into account the intracranial pulsations due to the heartbeats and, thus, fails to address the possible role of the pulsations in the development of hydrocephalus [4,32].

In this paper, we will assume that *the brain parenchyma is made of a nonlinear hyperelastic material and use the real geometry of the brain as it is shown in medical images taken from [10] to analyze the mechanical behavior of the brain.* We will examine *the effect of the ventricle pulsations and how these pulsations affect the development of hydrocephalus.* The finite element analysis is done using Abaqus/Standard version 6.8-2. We will show that *there exists a pressure threshold after which any increase in pressure due to pulsations will induce hydrocephalus.* **To the best of our knowledge, this is the first time such a mathematical and computational model is proposed for modeling, simulating, and studying hydrocephalus.**

2. BRAIN PARENCHYMA MODEL

2.1. Material Properties

We assume that the brain parenchyma behaves as an incompressible, isotropic hyperelastic material of the Mooney-Rivlin type. The general strain energy function of the Mooney-Rivlin material is given by [21]:

$$\Sigma(I_1, I_2) = \frac{\alpha}{2}(I_1 - 3) + \frac{\beta}{2}(I_2 - 3) \quad (1)$$

The Mooney-Rivlin strain energy function implemented in Abaqus has the following more general form [1]:

$$U = C_{10}(\bar{I}_1 - 3) + C_{01}(\bar{I}_2 - 3) + \frac{1}{D_1}(J^{el} - 1)^2 \quad (2)$$

where U denotes the strain energy per unit of reference volume, C_{10} , C_{01} , and D_1 are temperature-dependent material parameters, \bar{I}_1 and \bar{I}_2 are the first and second deviatoric strain invariants defined as:

$$\bar{I}_1 = \bar{\lambda}_1^2 + \bar{\lambda}_2^2 + \bar{\lambda}_3^2 \quad (4)$$

$$\bar{I}_2 = \bar{\lambda}_1^{(-2)} + \bar{\lambda}_2^{(-2)} + \bar{\lambda}_3^{(-2)} \quad (5)$$

where the deviatoric stretches $\bar{\lambda}_i = J^{-1/3} \lambda_i$; J is the total volume ratio; J^{el} is the elastic volume ratio; and λ_i are the principal stretches.

The constants C_{10} and C_{01} were taken from [7] and can be seen in Table 1. For our model the constant parameter D_1 was taken to be zero (due to the incompressibility constraint). The material parameters for the 5.08 mm/s strain rate were used in the model because hydrocephalus is a slow process which develops over an extended period of time. Therefore the slower strain rate material parameters were chosen in the model of the brain parenchyma.

Table 1: Mooney-Rivlin material parameters for different strain rates

Strain Rate [mm/s]	C_{10} [Pa]	C_{01} [Pa]
5.08	1585.8	620.5
50.8	965.3	4619.5
254	1861.6	5033.2

In Figure 2, we show that the constitutive model used for the brain parenchyma has a completely nonlinear representation throughout all the strain values.

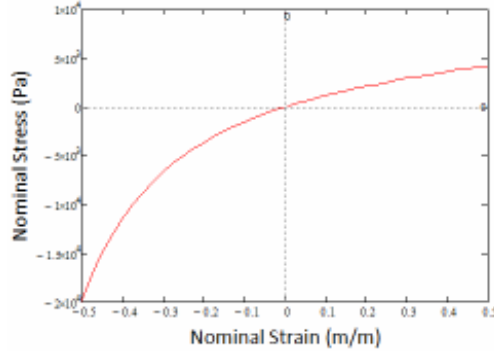


Figure 2: Stress vs. Strain plot, of the brain parenchyma, created by Abaqus' material evaluate tool. This plot corresponds to the Mooney-Rivlin material parameters, in Table 1, for a strain rate of 5.08m/s.

2.2. Geometry

The geometry of the brain parenchyma plays an important role in the brain's response to mechanical loading. As we can see in Figure 3a, the wavy nature of the cortical surface of the brain makes it difficult to create a realistic geometry of the brain directly in Abaqus. To insure an accurate geometry, a stack of MRI images were obtained from [10], in which image segmentation could be performed to create a data set importable into Abaqus. Two software packages called ScanIPTM and ScanFETM, from Simpleware Ltd. [11], were used to segment the brain parenchyma and generate a data set readable in Abaqus.

For simplicity, we chose to model just a thin slice off the brain. The model includes a 3mm thick slice, which was the minimum allowed by the image segmentation software.

In order to avoid any problems with the creation of the brain parenchyma mesh, we used a recursive Gaussian filter to smooth out the cortical surface and then manually created the vertical slots within the image segmentation software. This mesh kept the main geometric features of the brain and allowed the analysis in Abaqus to be done without any problems and should not affect the stress-strain analysis.

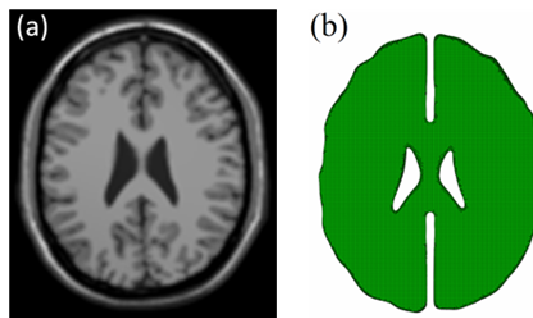


Figure 3: (a) One slice of a MR image. (b) 3mm thick mesh of the brain parenchyma, created by segmenting the image data shown in (a).

During the analysis, the geometric nonlinearity of the brain parenchyma was accounted for by turning on the NLGEOM feature within Abaqus.

2.3. Boundary Conditions

We will focus on the development of hydrocephalus in young adults (this is not normal pressure hydrocephalus). The outer cortical surface, excluding the vertical slots shown in Figure 3(b), was constrained to prevent any outward displacement of the brain parenchyma. This constraint is due to the rigidity of the adult skull. The top and bottom surfaces of the brain slice were also restrained from any displacement normal to the surface. This was done to mimic a plane stress model. A pulsatile pressure was applied to the outer surface of the ventricular walls to imitate the pulsations of brain due to the heartbeats [16]:

$$a(t) = \alpha \left(1.3 + \sin\left(\omega t - \frac{\pi}{2}\right) - \frac{1}{2} \cos\left(2\omega t - \frac{\pi}{2}\right) \right) \quad (6)$$

In our simulations we used the following parameters: $\alpha = 2500\text{Pa}$, $\omega = 1\text{Hz}$.

3. RESULTS

In Figures 4, 5, and 6, we show contour plots of the horizontal and vertical displacements at different ventricular pressures. The normal intracranial pressure in adults varies from approximately 780Pa to 1170Pa. Intracranial pressure values above 1960Pa in adults suggest the presence of hydrocephalus [14].

The size of the lateral ventricles shows a 10-20% change during the cardiac cycle as measured from medical images [14]. One of the base horizontal distances in the middle of the left ventricle is 1.16cm. During the cardiac cycle, this distance has a 1.16mm -2.32mm change. In our model, when a ventricular pressure of 1,013Pa is applied, to mimic the normal pressure within the brain, the ventricle horizontally expands 1.5mm, which is between the above mentioned normal limits. With a pressure of 2,549Pa the horizontal expansion is 3.86mm and for 5,886Pa the horizontal expansion is 5.04mm. This is a clear indication of the presence of hydrocephalus for pressures above 1960Pa. Contour plots of the Mises stresses at different ventricular pressures are shown in Figure 7.

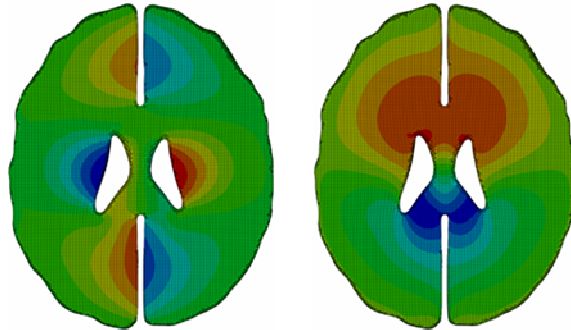


Figure 4: Horizontal displacements (limits: red = +1.104mm and blue = -1.089mm) (left) and vertical displacements (limits: red = +0.9325mm and blue = -1.392mm) (right) with a ventricular pressure of 1,013Pa.

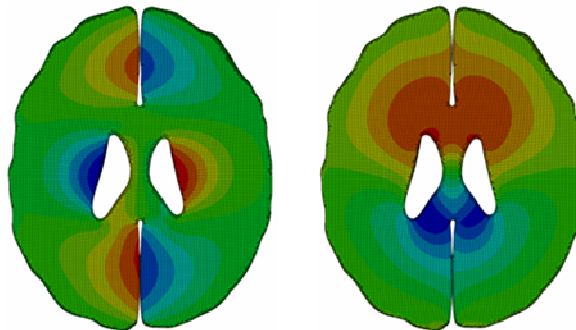


Figure 5: Horizontal displacements (limits: red = +2.713mm and blue = -2.67mm) (left) and vertical displacements (limits: red = +2.511mm and blue = -3.579mm) (right) with a ventricular pressure of 2,549Pa.

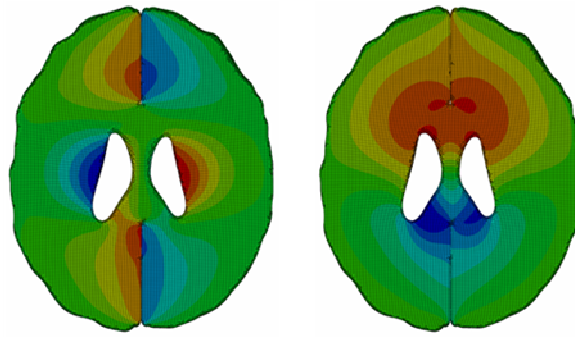


Figure 6: Horizontal displacements (limits: red = +3.529mm and blue = -3.456mm) (left) and vertical displacements (limits: red = +3.632mm and blue = -4.717mm) (right) with a ventricular pressure of 5,886Pa.

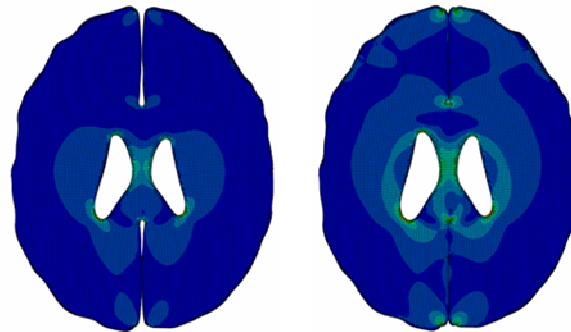


Figure 7: Mises Stress with a ventricular pressure of 2,549Pa (left) and with a ventricular pressure of 5,886Pa (right) (max stress = 28141.2Pa). (limits: red = 10865.8Pa and blue = 0Pa).

4. CONCLUDING REMARKS

In recent years, the biomechanics of brain parenchyma has been the subject of much interest in the literature. Mathematical models capable of correctly predicting the brain's response to mechanical loading induced by surgical procedures, trauma injuries, or conditions such as hydrocephalus, will help design better diagnoses, treatments, and protocols.

In this paper we modeled the brain parenchyma as an incompressible, isotropic, Mooney-Rivlin hyperelastic solid and used the real geometry of the brain as seen in medical images to analyze the response of the brain to pulsatile ventricular pressure. We have shown that for pressure values above 1960Pa the model correctly predicted large displacements of the ventricles of about 3-5mm. This means that once a pressure threshold of 1960Pa has been reached, any further pressure increase due to the pulsations will induce hydrocephalus. This is in agreement with clinical observations reported in [14].

In order to fully understand the mechanics of the brain, the presence of CSF inside the brain's ventricles and in the region between the brain parenchyma and the skull must be considered. Thus, in our further work we plan to study the interactions between the brain parenchyma and the ventricular CSF by adding to our model of the brain parenchyma the CSF dynamics. We expect that this improved model will provide better boundary conditions and enable us to predict the very large displacements seen in cases of fully developed hydrocephalus (Figure 1(b)).

In addition, we will continue our investigation into getting better, more anatomically correct meshes of the brain. The final goal is to obtain a three-dimensional mathematical model of the brain biomechanics capable of predicting the brain response to different mechanical loading.

REFERENCES

- [1] Abaqus Analysis User's Manual (v6.8-2) 18.5.1 Hyperelastic behavior of rubberlike materials.
- [2] Aschoff, A., Kremer, P., Hashemi, B., Krunze, S. 1999. The Scientific History of Hydrocephalus and its Treatment, Neurosurg.Rev. 22, 67-93.

- [3] Beatty, M.F. 1987. Topics in Finite Elasticity: Hyperelasticity of Rubber, Elastomers, and Biological Tissues- with Examples, *Appl.Mech.Rev.* 40(12), 1699-1734.
- [4] Bering, E. 1962. Circulation of the Cerebrospinal Fluid: Demonstration of the Choroid Plexuses as the Generator of the Force for Flow of Fluid and Ventricular Enlargement, *J. Neurosurg.* 19, 405–413.
- [5] Centers for Disease Control and Prevention, National Center for Health Statistics. 2003. <http://www.cdc.gov/nchs/releases/news/lifeex.htm>
- [6] Drake, J.M., Sainte-Rose, C. 1995. *The Shunt Book*, Blackwell Science Inc.
- [7] Drapaca, C., Tenti, G., Rohlf, K., Sivaloganathan, S. 2006. A Quasi-linear Viscoelastic Constitutive Equation for the Brain: Application to Hydrocephalus, *J. Elasticity* 85, 65-83.
- [8] Gjerris, F., Borgesen, S.E. 1992. Current Concepts of Measurement of Cerebrospinal Absorption and Biomechanics of Hydrocephalus, *Adv.Tech.Stand. Neurosurg.* 19, 145-177.
- [9] Hakim, S., Venegas, J., Burton, J. 1976. The Physics of the Cranial Cavity, Hydrocephalus and Normal Pressure Hydrocephalus: Mechanical Interpretation and Mathematical Model, *Surg. Neurol.* 5, 187–210.
- [10] <http://www.bic.mni.mcgill.ca/brainweb/>
- [11] <http://www.simpleware.com/index.php>
- [12] <http://www.e-radiography.net/ibase5/Brain/index.htm>
- [13] Hydrocephalus Statistics. 2008. <http://www.ghrforg.org/faq.htm>
- [14] Iantosca, M. 2009. private communication.
- [15] Kaczmarek, M., Subramaniam, R., Neff, S. 1997. The Hydromechanics of Hydrocephalus: Steady-State Solutions for Cylindrical Geometry, *Bull. Math.Biol.* 59, 295–323.
- [16] Linninger, A., Tsakiris, C., Zhu, D., Xenos, M., Roycewicz, P., Danziger, Z., Penn, R. 2005. Pulsatile Cerebrospinal Fluid Dynamics in the Human Brain, *IEEE Transactions on Biomedical Engineering* 52(4), 557-565.
- [17] Mendis, K., Stalnaker, R., Advani, S. 1995. A Constitutive Relationship for Large Deformation Finite-Element Modeling of Brain-Tissue, *J. Biomech. Eng.Trans. ASME* 117, 279–285.
- [18] Milhorat, T.H. 1978. *Pediatric Neurosurgery*, Contemporary Neurology Series 16.
- [19] Miller, K., Chinzei, K. 1997. Constitutive Modelling of Brain Tissue – Experiment and Theory, *J. Biomech.* 30, 1115–1121.
- [20] Miller, K. 1999. Constitutive Model of Brain Tissue Suitable for Finite Element Analysis of Surgical Procedures, *J. Biomech.* 32, 531–537.
- [21] Mooney, M. 1940. A Theory of Large Elastic Deformation, *J.Appl.Physics* 11, 582-593.
- [22] Nagashima, T., Tamaki, N., Matsumoto, S., Horwitz, B., Seguchi, Y. 1987. Biomechanics of Hydrocephalus: A New Theoretical Model, *Neurosurg.* 21 (6), 898–904.
- [23] Netter, F.H. 1972. *The CIBA Collection of Medical Illustrations: Nervous System*, CIBA.
- [24] Pena, A., Harris, N., Bolton, M., Czosnyka, M., Pickard, J. 2002. Communicating Hydrocephalus: the Biomechanics of Progressive Ventricular Enlargement Revisited, *Acta Neurochir.* 81, 59–63.
- [25] Relkin, N., Marmarou, A., Klinge, P., Bergsneider, M., Black, P. 2005. Diagnosing Idiopathic Normal Pressure Hydrocephalus, *Neurosurgery Online*, 57 (suppl.3), S4-S16.
- [26] Smillie, A., Sobey, I., Molnar, Z. 2005. A Hydroelastic Model of Hydrocephalus, *J. Fluid Mech.* 539, 417–443.
- [27] Tenti, G., Sivaloganathan, S., Drake, J.M. 1999. Brain Biomechanics: Steady-State Consolidation Theory of Hydrocephalus, *Can. App. Math. Q.* 7 (1), 111–124.
- [28] Tully, B., Ventikos, Y. 2009. Coupling Poroelasticity and CFD for Cerebrospinal Fluid Hydrodynamics, to appear in *J. Transactions on Biomedical Engineering*.
- [29] Vacca, V. 2007. Diagnosis and Treatment of Idiopathic Normal Pressure Hydrocephalus, *J.Neurosci.Nurs.* 39(2), 107-111.
- [30] Wang, H., Wineman, A. 1972. A Mathematical Model for the Determination of Viscoelastic Behavior of Brain in vivo. I. Oscillatory Response, *J. Biomech.* 5 (5), 431–446.
- [31] Wilkie, K., Drapaca, C., Sivaloganathan, S. 2009. A Theoretical Study of the Effect of Ventricular Pressure Pulsations on the Pathogenesis of Hydrocephalus, submitted to *Appl Math Comput*.
- [32] Wilson, C., Bertan, V. 1967. Interruption of the Anterior Choroidal Artery in Experimental Hydrocephalus, *Arch. Neurol.* 17 (6), 614–619.
- [33] Zhang, J., Williams, M.A., Rigamonti, D. 2006. Genetics of Human Hydrocephalus, *J.Neurol.* 253, 1255-1266.